Metallurgical
Science and Technology

A journal published
by Teksid Aluminum
twice a year

Vol. 21 No. 1, June 2003

Toughness characteristics of AS-die-cast AM60B alloy

E. Gariboldi, A. Lo Conte - Politecnico of Milano - Dipartimento di meccanica

TOUGHNESS CHARACTERISTICS OF AS-DIE-CAST AM60B ALLOY

E. Gariboldi, A. Lo Conte - Politecnico of Milano - Dipartimento di meccanica

Abstract

The present paper report on an experimental study on the toughness characteristics of the Mg-Al-Mn high purity alloy AM60B, that combines rather good ductility, casting properties and corrosion resistance. Today large thin section components for the automotive industry made of this alloy are industrially produced on large scale. In this context, the need of experimental data on toughness properties of this alloy in its specific microstructtural conditions with which the parts are serviced, i.e. in thin-section as die-cast components, is clear.

A set of experimental fracture toughness tests was carried out at room temperature on specimens machined directly from component produced on large scale in a high pressure cold-chamber machine. During each test the crack propagation was monitored via a potential drop method combined by the classical Johnson calibration equation, after checking its suitability by means of fractographic measurements of crack length at the end of tests. Crack growth resistance curves (R-curves) were obtained for several specimens of thickness in 2.5-3.1 mm range. No effect of specimen thickness was observed. The stress intensity factor leading to unstable crack propagation was determined for each specimen, being of about 20 MPam$^{1/2}$.

This crack extension properties of die-cast components are reasonably related not only to the chemical composition and microstructure of the alloy (this latter severely affected by cooling conditions), but also to the presence of defects such as inclusions or porosities and to temperature. The results obtained in the present experimental research, in particular the critical stress intensity factor, will thus be useful to compare the effects of different process parameters or of heat treatments or to check the effect of temperature, not as an absolute values of toughness easily extendable to thicker components.

Riassunto

Questo lavoro riporta i valori sperimentali di tenacità di campioni della lega del sistema Mg-Al-Mn denominata AM60B ad elevata purezza, generalmente caratterizzata dalla favorevole combinazione di duttilità, di colabilità e di resistenza alla corrosione. Queste leghe trovano oggi largo impiego nel campo dei componenti automobilistici piatti di grandi dimensioni con spessori sottili. In questo contesto risulta chiara la necessità di avere informazioni sulle proprietà delle leghe nella condizione microstrutturale di impiego cioè come parti a parete sottile nelle condizioni come pressocolati.

Una serie di prove di tenacità a temperatura ambiente è stata condotta su campioni ricavati dalla dissezione di componenti prodotti in larga scala con la tecnologia della pressocolata in camera fredda. Durante ogni prova la propagazione della cricca è stata controllata attraverso un metodo di caduta di potenziale combinato con la classica equazione di calibrazione di Johnson, dopo averne valutato la appropriatezza attraverso la misura della lunghezza della cricca alla fine delle prove. Le curve di resistenza alla propagazione della cricca (R-curves) sono state ottenute per diversi campioni di spessori compresi tra i 2,5 ed i 3,1 mm. Non è stata osservata alcuna influenza dello spessore sui risultati. Il fattore di intensificazione degli sforzi, che determina l'instabilità della propagazione della frattura è stato valutato per ogni campione, ed è risultato essere circa 20 MPa m$^{1/2}$.

Le proprietà di propagazione della frattura dei componenti pressocolati sembrano dipendere oltre che dalla composizione chimica e dalla microstruttura della lega (quest'ultima è pesantemente influenzata dal ciclo di raffreddamento), anche dalla presenza di difetti quali inclusioni e porosità, e dalla temperatura.

I risultati ottenuti da questa sperimentazione, in particolare il fattore di intensificazione degli sforzi, possono essere utili per confrontare gli effetti di variazioni dei parametri di processo o di trattamenti termici o per valutare l'effetto della temperatura. Non possono essere invece considerati come valori assoluti di tenacità estendibili a componenti di maggior spessore.

INTRODUCTION

The amount of parts made up of magnesium alloys rapidly increased during the nineties due to their opportunity of recycling and, above all, due to their reduced density that makes magnesium a desirable material for the automotive industry, since the car weight reduction is one of the most effective features to reach the strict targets on CO_2 emissions by 2010 [1, 2]. High purity magnesium die casting alloys have in particular attracted the attention of industry due to the combination of good fluidity, low specific heat per unit volume, limited tendency to sticking to dies. These properties make magnesium suitable for die-casting process, by means of which thin-walled parts of complex shapes can be manufactured [3-6]. These positive characteristics for die-cast process overbalance the well-known effects of the reactivity of the metal with oxygen that imposes the use of specific atmospheres in contact with the molten metal, and thus the use of dedicated die-casting machines [7,8]. The result is the soaring of the amount of die-cast magnesium components produced at reasonable costs every year (in 2001 the predicted amount was 120000t [1]).

Among the possible alloying elements for magnesium, aluminium and zinc, within proper limits, impart both strength and ductility with a concurrent improvement in castability. Manganese is also added in Mg-Al-Mn alloys to

improve corrosion properties. It is not surprising that these alloys (especially the AM60B) and Mg-Al-Zn-Mn alloys (especially the AZ91D) represent together more than 90% of the current structural applications of magnesium. Anyway, toughness properties of AZ91D do not match requirements for some components; for 'internal' car parts such as seat components, steering wheels core and instrument panel. AM60 and AM50 alloys, combining rather good ductility with good casting properties and corrosion resistance, are often the preferred materials [6]. Their share among die-casting alloy was foreseen to increase from 19 to 28% between 1997 and 2002 [2].

In this context, the need of experimental data on the toughness properties of AM60 alloy in the specific microstructural conditions with which the parts are serviced, i.e. in thin-section, often as die-cast components, is clear. Nevertheless, in the author's knowledge there are a few papers dealing with fracture toughness on AM60 alloy. As for other materials toughness properties of magnesium die-cast alloys are often compared on the basis of the energy absorbed in impact tests [9-11]. Using standard-size cast-in Charpy V notched specimens, the better toughness of AM60 with respect to AZ91 alloy was confirmed by higher absorbed energies (3.1 J and 1.4 J for the Mg-Al-Mn and Mg-Al-Zn alloy, respectively, [9]).

It should be pointed out that tests reported in literature either are performed on specimens machined from die-cast parts, the thickness of which rarely reach 5 mm, or are carried out using standard impact toughness specimens (10 mm thick) under different metallurgical and stress-state conditions. Results are thus not easily comparable. For example, in the case of AM60 alloy literature impact toughness data are available also for specimens having 0,07 mm machined notch on specimens 4.53 x 4.53 x 25.4 mm^3 (0.60-0,87 J) [10], on 3 mm thick Charpy V-notched specimens (0.73J) [11].

Similar reasoning need to be made when dealing with fracture toughness characteristics, since they depend on both microstructural features and stress state. With respect to fracture toughness data, it should be taken into account that the usual thickness of die-cast magnesium components is below the minimum required by ASTM standards to guarantee the existence of plane strain conditions, unless to perform tests on miniaturized specimens. On the other hand, the use of thicker components for carrying out experimental tests would correspond to different microstructural characteristics of the material and, thus, to different mechanical and toughness properties. It is thus reasonable, for industrial die-cast parts produced on large scale, to evaluate fracture properties for common thickness (and microstructure), approaching plane stress condition. Results will thus be useful to compare different alloys as well as the effects of process parameters or heat treatments or to temperature, even if they will not be easily extendable to thicker components.

Following this line, a detailed investigation was carried out to define the progressive extension of the crack under increasing load, to obtain R-curve and to check if a critical stress intensity factor can be defined for material taken from industrial components produced in a high pressure cold-chamber machine.

MATERIALS AND EXPERIMENTS

The present investigation was carried out on an high-purity magnesium alloy, AM60B, the specified composition of which is given in Table 1.

Table 1. Specified chemical composition (% by mass) of AM60B alloy

Al	Mn	Cu	Ni	Fe	Si	Zn	Mg	
AM60B	5.5-6.5	0.25-0.5	<0.01	<0,002	<0.005	<0.1	<0.22	Bal.

The material was supplied as rectangular plates machined from a batch of large-scale die-cast parts produced by means of a cold-chamber machine, leaving unaltered the thickness of about 3 mm, almost constant in the sampling zone.

Due to the thickness of the plates, even for the quite low plane-strain fracture toughness elsewhere reported for magnesium alloys (K_{IC}=15,22 MPa $m^{1/2}$ for AZ91 alloy [12]), and for yield stresses (σ_Y) reported in literature [11], the minimum thickness ($B=2.5*(K_{IC}/\sigma_Y)^2$), one of the conditions required by ASTM E399-97 Standard [13] for measurement of critical stress intensity factor under plane strain conditions was not satisfied. The use CT specimens for determining the fracture toughness according to ASTM E1820-99a would have required excessive specimen miniaturization since, even considering a W/B of 4, for B equal to 2.5mm W would have been 10 mm in the case of CT specimens.

Following what proposed in ASTM B 646 [15] standard for quality assurance purposes in the case of aluminium alloys products in thin sections, the measurement of critical stress intensity factor (K_c) associated with a monotonically loaded centre-slotted or cracked M(T) panel tested in accordance to ASTM E 561 Standard [16] was chosen for the present experimental study. The ASTM E 561 standard provides indications to draw R-curve, the continuous record of toughness development (in terms of crack extension resistance K_R) as a function of crack length as the stress intensity factor increases. This allows the determination of

plane stress fracture toughness (K_c) as the K_R value at the instability condition determined from the tangency between the R-curve and the applied stress intensity factor for the specimen (K-curve). ASTM B 646 Standard includes also the possibility to test M(T) specimens of reduced width in the case of insufficient material dimensions. It is worthwhile to mention that K_c will decrease with W, all other factors being identical [15]. Thus, comparisons on fracture toughness properties could be made on the basis of (almost) equal component thickness and specimen width.

Thus, middle cracked tension M(T) specimens having a length (L) of 95 mm, a width (W) of 33 mm were obtained from the supplied plates. Their thickness (B), left unmachined, ranged between 2.48 and 3.10 mm (see Table 2) for the specimens used in experiments reported in the present paper. The central notch was a drilled buttonhole notch, 6 mm long, 1 mm wide. The specimens were fatigue pre-cracked using the procedure that will be explained later. The geometry proportions required by ASTM E 561 standard on specimen size, notch and fatigue precrack length were satisfied for the chosen width value.

In order to carry out potential drop data acquisition for indirect measurement of crack displacement, two clearance holes of diameter 1 mm were symmetrically drilled along the longitudinal axis of the specimen, 3.5 mm centre-to-centre distance from the buttonhole notch. To carry out remote potential drop measurements in some specimens, two additional holes of the same diameter were placed 7 mm centre-to centre distance at 3 mm from the lateral surface of the specimen, the nearer being at 12 mm distance from the plane of buttonhole notch (Figure 1). Potential drop measurements were made using a DC potential drop system supplying a constant 20 A current by means of multiple-wires copper input probes tightened in contact to the specimen ends by the gripping system. The potential drop signals was monitored by means of an 5.5 digit multimeter at an acquisition frequency of 1 Hz.

Each specimen was mounted in the gripping system shown in Figure 1 and placed on an INSTRON 8501 universal testing machine to perform fatigue precracking, immediately followed by crack extension test. Precracking was carried out in two

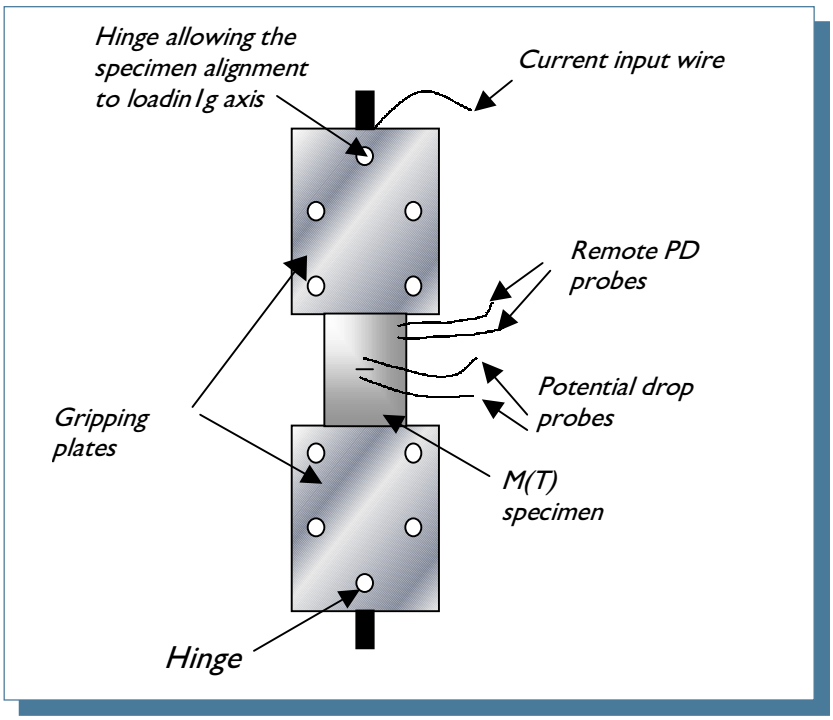

Fig. 1: Scheme of M(T) specimen mounted in the gripping system, equipped with current input and potential drop measurement wires. Such gripping system was used on a universal testing machine to perform precracking, immediately followed by crack extension test.

steps, at a frequency of 5 Hz, using a load range 0.1-5 KN in the first step (about 17000 cycles), a 0.1-3 KN range (0.1-2 KN for thinner specimens) in the second step. The number of cycles of this latter varying between 2000 and 3000.

After precracking, the test to define the crack extension resistance (K_R) curve of the material was performed by step increasing the tensile load applied to the specimen and by recording potential drop as done during pre-cracking. During each load step the load was increased in 10s and hold for 60s in order to stabilize, before occurrence of unstable propagation, the crack length. Each test ended with the occurrence of unstable propagation of the crack. The design of the load history was also made taking into account the real thickness of specimens and the load increments at each step decreased as the load increased in order to obtain a greater density of experimental points on the R-curve.

Due to the reduced stiffness of the thin magnesium alloy specimens, the possibility of developing buckling during the test was carefully considered. As described in ASTM E 561, two tests were carried out on the same specimen (A3 specimen, having B 3.00 mm) with and without a device for buckling restrain placed on its central portion. The crack opening displacement at increasing load was measured by means of a strain gauge placed across the crack and by means of optical observations. As illustrated in Figure 2, the loading-unloading curves with and without the abovementioned device overlap and thus experimental tests were carried out without it.

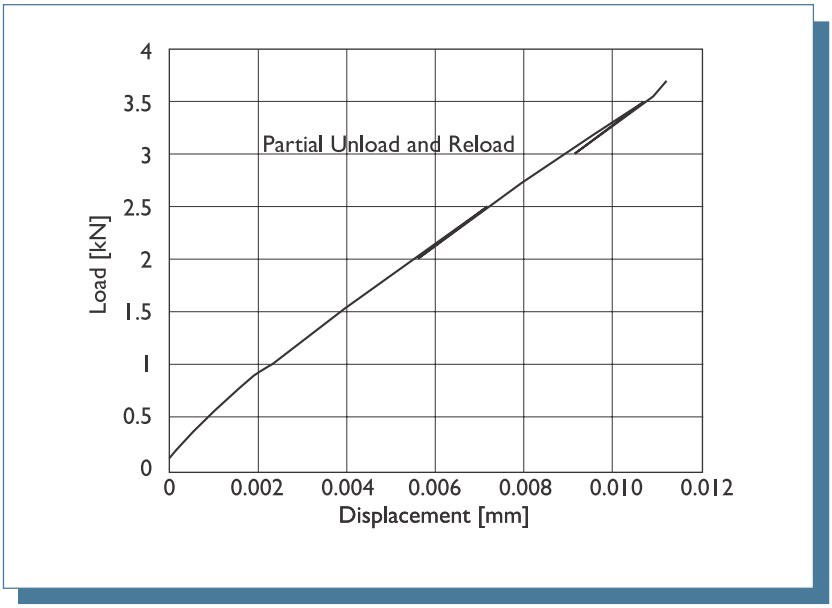

Fig. 2: Loading-unloading curves with and without the device to retain buckling.

In the present invstigation the well-known Johnson's calibration curve for M(T) specimens [16] was used to correlate the recorded potential drop across the crack to the physical crack length (a_p) and to its measured initial value. At the end of experimental tests, the actual values of notch length (a_n), physical length of precrack (referred also as initial crack length (a_o) and final physical crack length at the end of the test $(a_{f,m})$ were measured using SEM fractographs (25X) as average of 11 values taken at equal distances along the specimen thickness on each side of the notch. The crack length measurement on a stereomicroscope at 50X was also tried, but the definition of the final crack length gave rise to greater uncertainties. The symmetry of notch and crack was checked to be within the limits allowed by ASTM E 561 Standard and the average values were used for the calculation of fracture toughness properties.

Scanning electron microscopy metallographical and fractographical observations on fractured specimens completed the experimental analyses. A different specimen was machined from the plates to perform a tension test. Its gauge length was 25 mm and its cross section was 15 x 2.96 mm^2; each gripping end was 25 mm long and 35 mm wide, connected to the gauge length by a region with 10 mm radius. Tensile tests were performed at room temperature under displacement control at an initial strain rate of 6.7×10^{-4} 1/s. An extensometer of gauge length 25 mm was used to obtain both Young's modulus and 0.2% offset yield stress.

Table 2. Geometry of M(T) specimens and average a/W ratios corresponding to notch length (a_N) initial (a_o) and final measured ($a_{F,M}$) crack lengths. Critical stress intensity factors K_c and radius of the plastic zone r_y (corresponding to the last point plotted on R-curves) are listed in the last columns

SPECIMEN	W (mm)	B (mm)	a_n/W	a_o/W	$a_{f,m}/W$	$(a_{f,j}/W)$	$(a_{f,exp}/W)$	K_c (MPa $m^{1/2}$)	r_y (mm)
A1	3276	3.10	0.091	0.130	0.155	0.160	0.167	19.75	3.95
A20	33.07	3.075	0.091	0.172	0.179	0.179	0.172	20.00	3.25
A17	32.88	2.92	0.092	0.141	0.165	0.163	0.160	19.85	4.73
A19	33.23	2.94	0.090	0.126	0.147	0.137	0.144	19.70	4.76
A10	33.42	2.67	0.090	0.206	0.240	0.242	0.249	19.83	4
A11	33.18	2.48	0.090	0.206	0.250	0.239	0.238	19.65	4.43
A9	33.35	2.58	0.090	0.211	-	-	-	-	-

RESULTS AND DISCUSSION

The tensile properties obtained from the test performed on a specimen of this batch are the following: Young's modulus (E) 42925 MPa, yield stress (σ_Y) 116 MPa, ultimate tensile stress (UTS) 229 MPa and a final elongation of 8.5%%. These data were well within the range of data reported in literature for AM60B alloy in cases of similar ductility [11, 12, 18].

The experimental data in terms of potential drop vs. time (an example is given in figure 2) were elaborated to obtain the stabilized potential drop values corresponding to each load step.

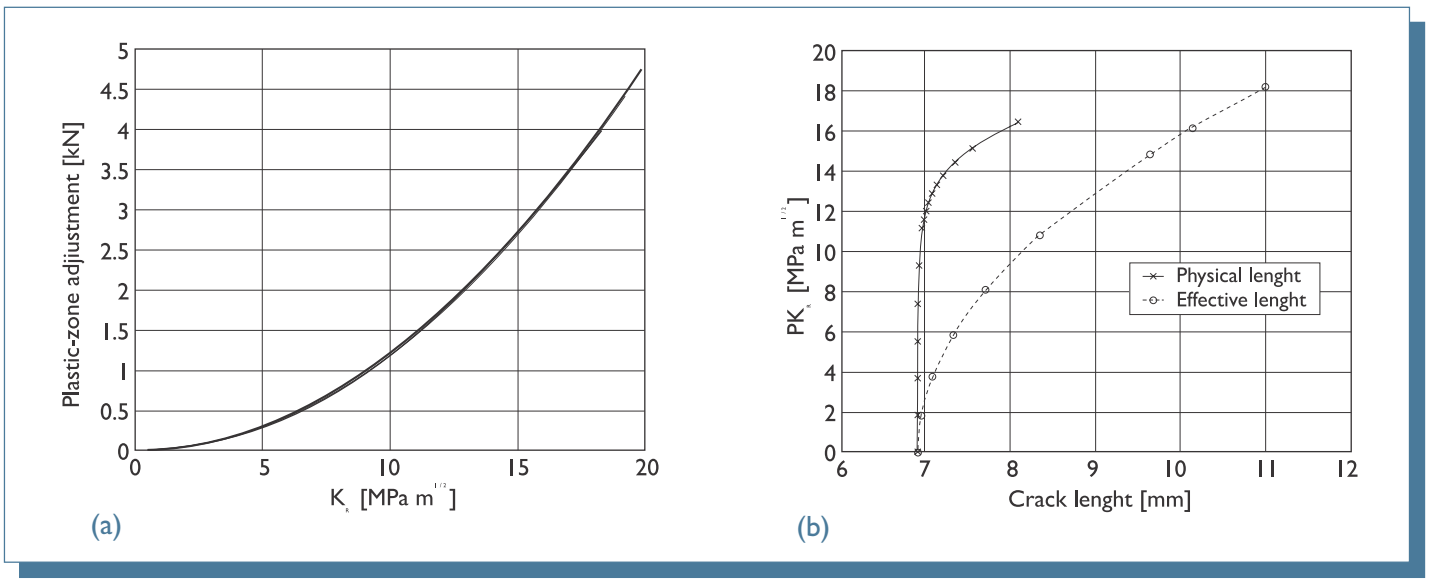

Fig. 2: Experimental applied load history (a) and corresponding curve of PD measurements (b) for specimen A10 (see Table 2).

The *2a/W* ratios corresponding to the initial notch ($2a_n/W$), to precrack ($2a_f/W$) and final crack length ($2a_f/W$) obtained by measurements on fracture surfaces are listed in Table 2. The 2a/W ratios corresponding to the final crack length evaluated by means of the calibration formulae proposed by Johnson [16], inserting in it the PD value corresponding to load step at which specimen fracture occurred are listed in the same table. Final ligament lengths experimentally measured by optical and SEM observations were compared to those computed using the abovementioned calibration in $(PD*B*W/I)$ vs. $(1-2a/W)^{-1}$ diagram plotted in Figure 3. The $(1-2a/W)^{-1}$ values computed from final crack lengths were generally close to those from measured lengths, for which the trend to align is clear. The trend line can be expressed in terms of *a-PD* correlation as:

$$2a = W*[1 - (0.0019*I)/(PD*B*W + 0.0013*I)] \quad (1)$$

when *W*, *a* and *B* are expressed in millimeters, *I* in Ampere and *PD* in Volt. Experimental scatter in the measurement of specimen geometry and final crack length as well as in the actual room temperature, made more convenient the use of Johnson calibration to evaluate the physical crack length corresponding to stabilized *PD* values. Using this calibration, the difference between measured and computed crack length exceed the 0.25 mm allowed by ASTM E 561 standard only for the final points on R-curve in two tests.

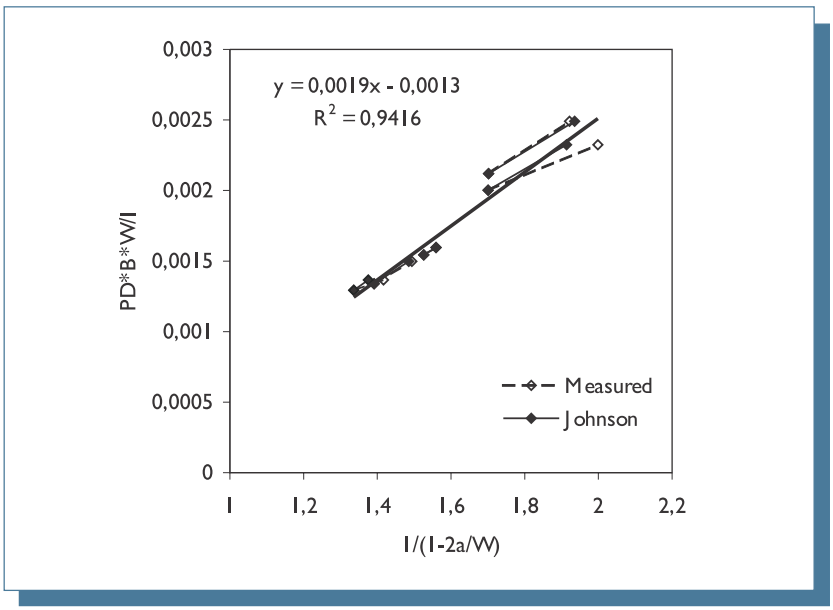

Fig. 3: Correlation between PD measurements and geometry of cracked specimens. The fitting curve could be considered as experimental calibration curve.

For this purpose, for each load level P and for the corresponding stabilized effective crack length a_{eff}, the K_R value was computed using the formula proposed for M(T) specimens in ASTM E 561 standard

$$K_R = \frac{P}{W \cdot B}\sqrt{a_{eff}} \cdot f\left(\frac{a_{eff}}{W}\right) \quad (2)$$

where the function f is as follows:

$$f\left(\frac{a_{eff}}{W}\right) = \left[1.77 - 0.177 \cdot \left(\frac{2a_{eff}}{W}\right) + 1.77\left(\frac{2a_{eff}}{W}\right)^2\right] \quad (3)$$

The effective crack length can be defined adding to the physical crack length (a) the radius r_y of the plastic zone to account for effects of crack-tip plasticization on the linear-elastic stress field. The evaluation of r_y was made on the basis of the correlation [15] for plane stress condition:

$$r_p = \frac{1}{2\pi} \cdot \left(\frac{K}{R_{p0,2}}\right)^2 \quad (4)$$

Since r_y, and thus a_{eff}, depend on the value of K, both a_{eff} and K were determined at each load level by numerically finding the zero of equation (2). The dependence of r_y on K is reported in Figure 4a for specimen A10. r_y becomes a relatively large fraction of the physical crack length (and of the ligament) above 14 MPa m$^{1/2}$, where effective and physical crack lengths can differ of more than 2 mm (Figure 4b).

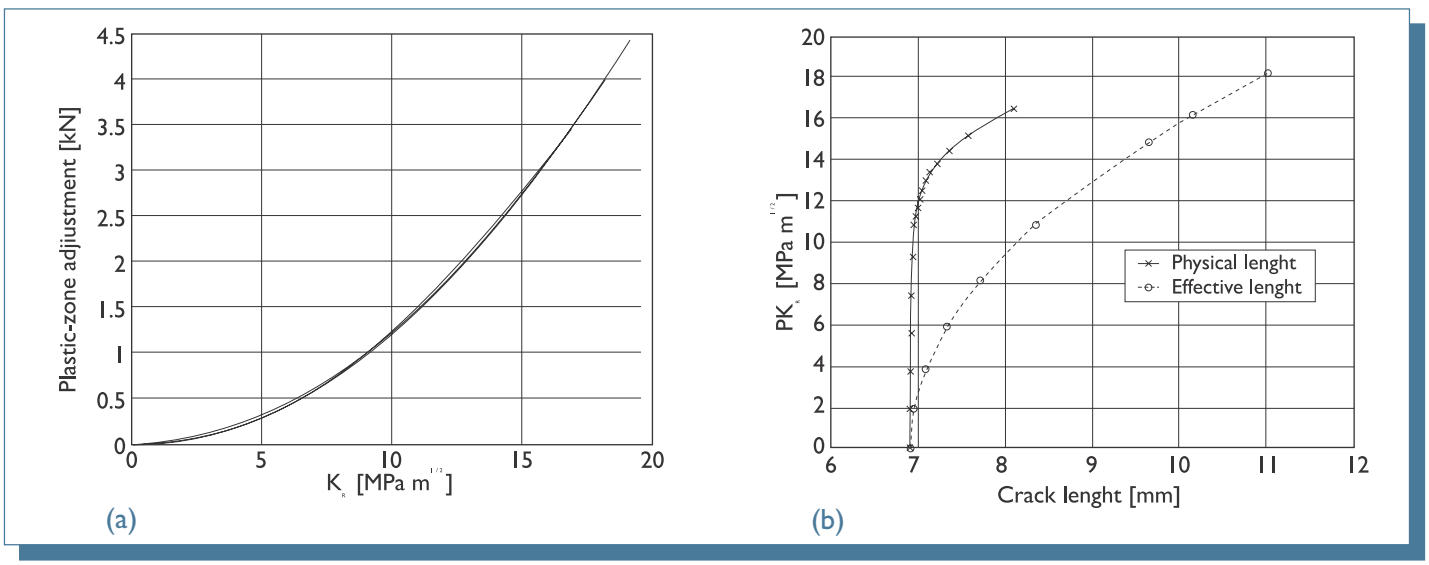

Fig. 4: Dependence of r_y values on K for specimen A1 (a). Different R-curves taking into account (effective crack length a_{eff}) or not (physical crack length a_{phys}) the plastic adjustment (b).

The predominance of elastic behaviour in the ligament for the validity of the K analysis according to ASTM E 561 was defined by tacking into account experimental points for which more than 50% of the ligament behave elastically. Mathematically this can be written as:

$$(W-2*a_{eff})/(W-2*a) < 0.5 \quad (5)$$

The r_y values corresponding to the last experimental a/W-K_R point taken into account for each specimen are listed in Table 2. The corresponding extension of plastic zone ranged between 35 and 46% for different specimens.

For each specimen the values of a_{eff} and K determined at different load level defined the crack extension resistance, or R-curve. The set of R-curves obtained for 6 specimens up to the load extending the plasticized zone less than half of the ligament (for example for specimen A10 only load step 1 to 9 shown in Figure 2 were used) is plotted in Figure 5 as function of effective crack extension. The crack growth resistance (K_R)curve is a material property and should not depend on specimen geometry. The curves obtained from the six experimental tests carried out on specimens of thickness in the range 2.48-3.10 mm perfectly overlap.

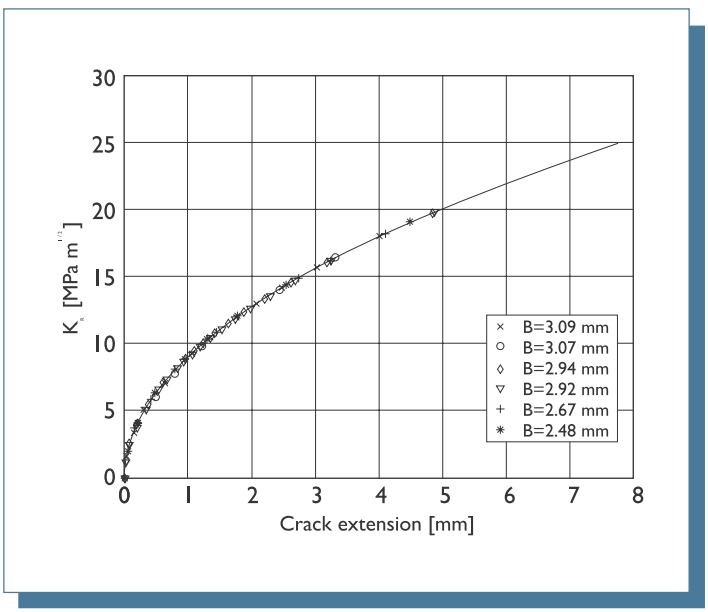

Fig. 5: Experimental R-curves plotted as function of effective crack extension (Δa_{eff}) for six specimens of slightly different.

Experimental data were fitted by the power-law curve plotted as continuous line in the same diagram. The equation of the fitted R-curve is:

$$K_R = 9.09\,(Da_{eff})^{0.4937} \quad (5)$$

Where K_R is expressed in MPa $m^{1/2}$ and Da_{eff} in mm.

For each specimen, the appropriate K_c instabiliy stress intensity factor was obtained following the classical procedure for load controlled tests, increasing the load level up to that for which R-curve vs. $2a_{eff}/W$ and K vs. $2a_{eff}/W$ curves are tangent. The results are visible in Figure 6 and listed in Table 2. The tangency was generally found for experimental points for which the condition in equation (5) was met, with the exception of specimen A20 for which an excessive load increase made necessary the use of fitted R-curve for K_c evaluation. The average K_c was of 19.8 MPa $m^{1/2}$ for all the specimens.

A further result of the present investigation was the opportunity to correlate the applied gross stress (defined as $P/(W-2*a_{phys})$ and a_{phys}, being a_{phys} the physical crack length corresponding to instable crack propagation, as presented in figure 7. Within the quite limited experimental gross stress range the correlation is linear and no effect of specimen thickness was observed. The extension of this correlation to different gross stress and specimen thickness is not immediate since, as reported in literature, the curve modifies for extended gross stress and specimen thickness ranges [18].

As previously observed, to the author's knowledge, presently there is a lack of toughness data published for this material, thickness and microstructural condition. Anyway, a comparison with data presented in papers for other thickness or other magnesium alloys may be of interest.

The fracture toughness of the alloy is at good level compared with K_{IC} in the range 15-22 MPa $m^{1/2}$ reported by Kleiner et al. [12] for the more extensively used AZ91 alloy (less ductile but with higher tensile properties than AM60 alloy), in as cast components obtained by squeezecasting and rheocasting processes that should improve toughness with respect to die-cast components. These values, reported were reasonably, according to ASTM 1820 standard, K_Q values, for specimen thickness in the 2-14 mm range stated by authors, too small for determining K_{IC} values.

For the same as die-cast AM60B alloy Iskander et al. evaluated material toughness in terms of J_Q, the value of which was 11-12 kJ m^{-2}, for CT specimens

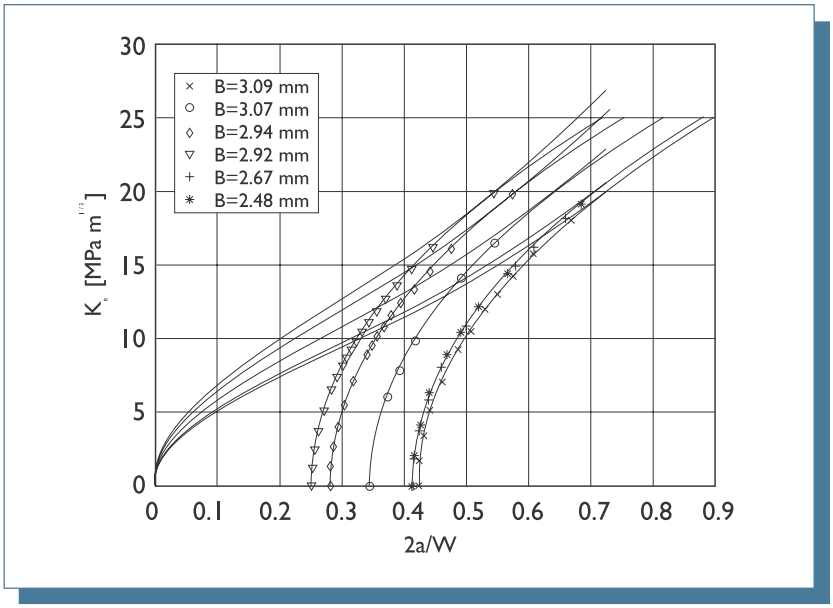

Fig. 6: K vs. $2a_{eff}/W$ curves to tangent to the corresponding crack extension resistence (K_R) vs. $2a_{eff}/W$ curves (both experimental data and lines corresponding to equation 3 are plotted).

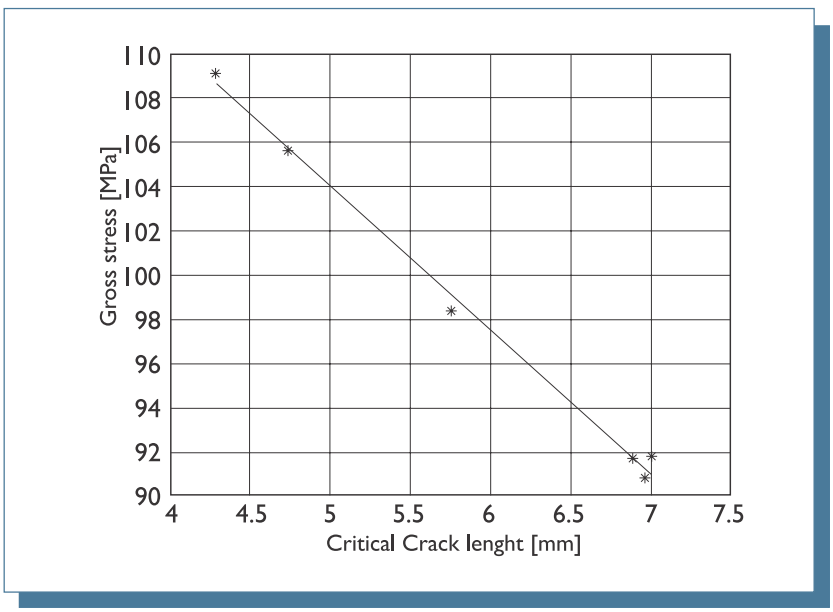

Fig. 7: Correlation between the applied gross stress and physical crack length leding to to instable crack propagation.

of about 5 mm (0.19 in) thickness that did not exhibited unstable fracture [19]. Due to the different approach, a real comparison between J_Q and K_R cannot be performed. Nevertheless, it can be observed that the elastic part of J total (computed as K^2/E for plane stress conditions) from the present experimental results is equal to 9.7 kJ m^2 and could match the abovementioned results in terms of J_Q. Deeper considerations about the comparisons between the results from the two approaches could not be done unless the size of plastic zone is not available.

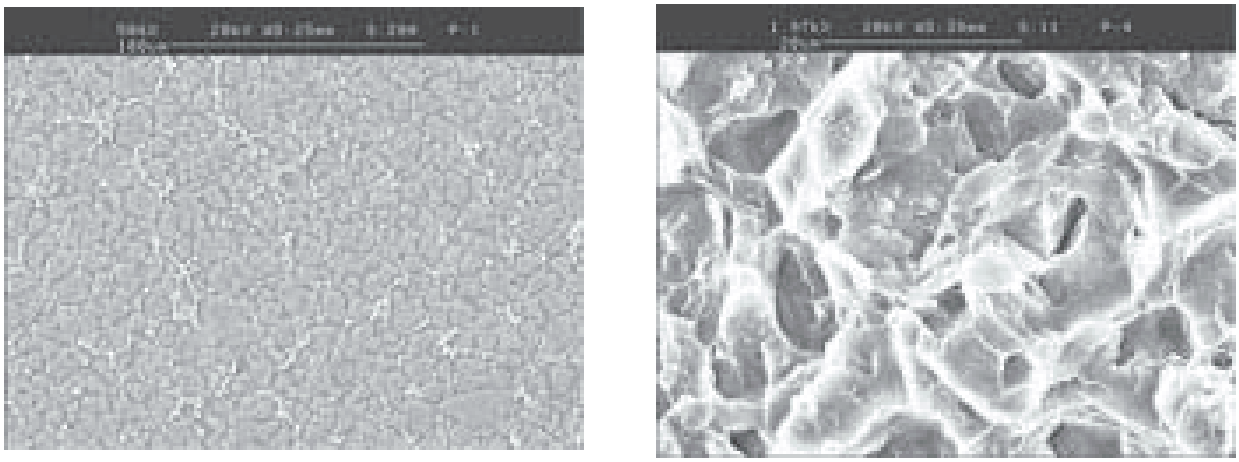

(a) (b)

Fig. 8: Microstructure of the bulk AM60B alloy in as die-cast specimens (a) and fracure surface in the region of crack extension during the test.

Micrographic observations showed the typical microstructural features of this Mg-Al-Mn alloy in the as-cast condition presented in Figure 8a. The fine grained structure (grain size is about 10 mm) is made up of a phase (solid solution of Al in Mg) surrounded by eutectic structure made up of a phase (richer in Al for microsegregation effect) and b phase ($Mg_{17}Al_{12}$ intermetallic). Some porosities located at grain boundaries are visible at higher magnifications. A slightly finer microstructure having the same microstructural features, correlated to an more rapid cooling process, was found on the external region of specimens.

The examination of the fracture surface in the region of crack extension during step loading (Figure 8b) revealed a rather ductile behaviour, with the crack propagation within α-phase. Some occasional cleavage facets and secondary cracks are also visible and some intermetallic β phase sometimes appears on the fracture surface. The fracture surface corresponding to final fracture substantially showed the same microstructural features, with slightly reduced plastic deformation.

This crack extension properties are reasonably related not only to the chemical composition and microstructure of the alloy (this latter severely affected by cooling conditions), but also to the presence of defects such as inclusions or porosities and to temperature. The results obtained in the present experimental research, in particular the critical stress intensity factor, will thus be useful to compare the effects of different process parameters or of heat treatments or to check the effect of temperature, not as an absolute values of toughness easily extendable to thicker components.

CONCLUSIONS

The toughness characteristics at room temperature of the AM60B alloy die-cast in thin section parts was experimentally evaluated in the as die-cast condition. For thickness of the order of experimental specimens (2.5-3 mm), the fitted curve of experimental data can be assumed as the R-curve of the examined die-cast alloy in the as cast condition. The stress intensity factor K_c leading to unstable crack propagation under predominantly elastic conditions in the ligament was determined, being of about 20 $MPam^{1/2}$. For the experimental component thickness and gross stress range a a linear correlation between this stress and the physical crack length at the occurrence of unstable propagation was observed.

ACKNOWLEDGMENTS

The authors wish to thank Meridian Magnesium Products of Italy (Verres, Italy) for the material supplied and eng. F. Antonuzzo for his help in carrying out the experimental work for the research presented in this paper.

REFERENCES

[1] B.L. Mordike, T. Ebert. Magnesium Properties, application, potential. Materials Science Engineering, A302, (2001), pp. 37-45.

[2] E. Aghion, B. Bronfin, D. Eliezer. The role of the magnesium industry in protecting the environment, J. Mater. Proc. Technol., 117 (2001), pp 381-385.

[3] I.J. Polmear, Magnesium alloys and applications. Mater. Sci. Technol., 1994, 10, (1), 1-16.

[4] P.D. Caton, New applications for magnesium die castings. In 'Magnesium alloys and their applications', (ed. B.L. Mordike), DGM Informationsgesellschaft, (1992), pp. 367-373.

[5] G.S. Cole, R.A. Finstad, J.C. Grebetz, The potential for magnesium in the automotive industry, Proc. Int. Conf. 'IMA52 – Magnesium perspective'. San Francisco, CA., May 1995, pp. 1-5.

[6] S. Schumann, F. Friedrich, The use of magnesium in cars - Today and in the future. In 'Magnesium alloys and their applications', (ed. B.L. Mordike, K.U. Kainer), Werkstoff Informationsgesellschaft mbH, 1998, pp. 3-13;.

[7] D.J. Sakkinen, Physical Metallurgy of Magnesium Alloys. SAE Technical paper 940779, SAE, Detriot, MI, 1994.

[8] O. Holta, H. Westengen, D. Albright, High Purity Magnesium Die Casting Alloys: From Ingot to cast Product. SAE Technical Paper 940413, SAE, Detriot, MI, 1994.

[9] T.K. Aune, H. Westengen, Property update on magnesium die casting alloys. In 'SAE Technical paper series', SAE Technical Paper 950424, SAE, Detriot, MI, 1995.

[10] S.K. Iskander, R.K. Namstad, S. Viswanathan, R.L. Swain, Fracture toughness of magnesium alloy AM60B. Magnesium Technology 2000, Ed. H.I. Kaplan, J. Hryn, B. Clow, The Minerals, Metals & Materials Society (2000), pp. 325-329.

[11] M. Vedani, C. Mapelli. Effect of thermal treatments on microstructres and impact toughness of die-cast Mg-Al-Mn alloys. Mater. Sci. Technol., 17 (2001), pp. 938-944.

[12] S. Kleiner, O. Beffort, A. Wahlan, P.J. Uggowitzer. Microstructure and mechanical properties of squeeze-cast and semi-solid cast Mg-Al alloys. J. Ligth Metals, 2 (2002) pp. 277-280.

[13] ASTM E 399-9-Standard. Test method for Plane-strain Fracture Toughness of Metallic Materials.

[14] ASTM E 1820-99a. Standard test method for measurement of fracture toughness.

[15] ASTM B 646-97. Standard Practice for Fracture Toughness Testing of Aluminium Alloys.

[16] ASTM E 561-98. Standard Practice for R-curve determination.

[17] H.H. Johnson, Calibrating the electrical potential method for studying slow crack growth., Material Res. Stand. (1965), p. 442-445.

[18] R.H. Heyer, D.E. McCabe, Crack growth resistance in plane-stres fracture testing. Eng. Fract. Mechanics, 4 (1972), pp. 413-450.

[19] S.K. Iskander, R.K. Nanstad, S. Viswanathan, R.L. Swain, J.F. Wallace. Fracture toughness of magnesium alloy AM60B. Proc. Conf. Magnesium Technology 2000, Ed. H.I. Kaplan, Hryn, B. Clow. The Metals, Metals and Materials Society, (2000), pp. 325-329.